2015

Triacylglycerol synthesis during nitrogen stress involves the prokaryotic lipid synthesis pathway and acyl chain remodeling in the microalgae *Coccomyxa subellipsoidea*

James W. Allen
University of Nebraska–Lincoln, jallen7@unl.edu

Concetta C. DiRusso
University of Nebraska-Lincoln, cdirusso2@unl.edu

Paul N. Black
University of Nebraska-Lincoln, pblack2@unl.edu

Published in *Algal Research* 10 (2015), pp 110–120. doi 10.1016/j.algal.2015.04.019

Submitted 25 November 2014; revised 24 March 2015; accepted 19 April 2015; published online 4 May 2015.

Triacylglycerol synthesis during nitrogen stress involves the prokaryotic lipid synthesis pathway and acyl chain remodeling in the microalgae *Coccomyxa subellipsoidea*

James W. Allen, Concetta C. DiRusso, and Paul N. Black

Department of Biochemistry, University of Nebraska–Lincoln

Correspondence: J. W. Allen, P. N. Black, University of Nebraska-Lincoln,
N236 GW Beadle Center, 1901 Vine Street, Lincoln, NE 68588-0664; jallen7@unl.edu , pblack2@unl.edu

Abstract

Triglyceride (TAG) synthesis during nitrogen starvation and recovery was addressed using *Coccomyxa subellipsoidea* by analyzing acyl-chain composition and redistribution using a bioreactor-controlled time course. Galactolipids, phospholipids and TAGs were profiled using liquid chromatography tandem mass spectroscopy (LC–MS/MS). TAG levels increased linearly through 10 days of N starvation to a final concentration of 12.6% dry weight (DW), while chloroplast membrane lipids decreased from 5% to 1.5% DW. The relative quantities of TAG molecular species, differing in acyl chain length and glycerol backbone position, remained unchanged from 3 to 10 days of N starvation. Six TAG species comprised approximately half the TAG pool. An average of 16.5% of the acyl chains had two or more double bonds consistent with their specific transfer from membrane lipids to TAGs during N starvation. The addition of nitrate following 10 days of N starvation resulted in a dramatic shift from chloroplast-derived to endoplasmic reticulum-derived galactolipids (from <12% to >40%). A model for TAG synthesis in *C. subellipsoidea* was developed based on the acquired data and known plant pathways and data presented.

Keywords: LC–MS/MS, Biofuels, Algae, *Coccomyxa subellipsoidea,* Triglycerides, Acyl editing, Triglyceride synthesis

Abbreviations: LC–MS/MS, liquid chromatography tandem mass spectroscopy; GC–MS, gas chromatography mass spectroscopy; TAG, triglyceride; MRM, multiple reaction monitoring; DAG, diacylglyceride; MGDG, monogalactosyl-diacylglyceride; DGDG, digalactosyl-diacylglyceride; PG, phosphatidylglycerol; PE, phosphatidylethanolamine; PC, phosphatidylcholine.

1. Introduction

Eukaryotic green algae accumulate triglyceride (TAG) at the expense of cellular reproduction while under abiotic stress (e.g., nitrogen, sulfur and iron deprivation) [1,2]. Recent studies using continuous cultures support this correlation by demonstrating a progression between reproductive growth and lipogenesis depending on the extent of the stress applied [3,4]. This correlation is not as obvious during less extreme stress conditions. In the case of reduced N deprivation, several reports in some algal species have shown an increased biomass [4,5]. These studies are consistent with a specific dissociation between growth and lipogenesis. It is precisely this dissociation that supports the generation and/or selection of an algal TAG production strain, which is essential and a key priority in algal biofuel research. In order to achieve this goal, it is first essential to gain a comprehensive understanding of metabolic changes leading to TAG synthesis in microalgae.

Genomic and transcriptional profiling show a number of algal species contain TAG synthesis, membrane lipid remodeling, and acyl chain editing genes that are homologous to known plant genes and further demonstrate differential expression patterns under conditions promoting TAG synthesis [6–10]. Phosphatidylcholine:diacylglycerol acyltransferase (PDAT) and the type-1 and type-2 diacylglycerol acyltransferases (DGATs), for example, are up-regulated under N starvation in *Chlamydomonas reinhardtii*. The role of PDAT in TAG synthesis has been confirmed by insertional mutagenesis [7]. While there are some changes in gene expression, the expectation of significant differential gene expression during N starvation has not been confirmed in proteomic studies. The levels of most lipid metabolic enzymes remain relatively constant during N stress [11–13] suggesting changes in their activities are likely the result of post-translational regulation as opposed to significant de novo protein synthesis. Metabolomic approaches, likewise, have been unable to completely address the specific metabolic processes and their relative importance leading to increased TAG synthesis [14–16].

Comprehensive studies addressing the metabolic processes underlying TAG synthesis in algae have lagged behind the phenotypic data showing oil accumulation during abiotic stress. In plants, TAG synthesis occurs through a complex and interwoven set of metabolic steps, which are organellar- and tissue-specific, many of which occur at specific points during development [17]. Chloroplast- and ER-specific isoforms of lysophosphatidic acid acyltransferase (LPAT) catalyze the addition of

palmitoyl-CoA or oleoyl-CoA, respectively, at the *sn*-2 position of the glycerol backbone to formphosphatidic acid, which is subsequently dephosphorylated by phosphatidic acid phosphatase (PAP) to form diacylglycerol (DAG) leading to distinctive pools of complex lipids [18]. TAG synthesis occurs in the ER from DAG and acyl-CoA, which is catalyzed by one of several isoforms of DGAT [19–21]. The Kennedy Pathway coexists with phosphatidylcholine:diacylglycerol acyltransferase (PDAT), which catalyzes the coenzyme A (CoA) independent acylation of DAG using phosphatidylcholine (PC) as the acyl donor, resulting in TAG and lyso-PC [22]. In developing soybeans, the primary acceptor of de novo synthesized fatty acid is lyso-PC resulting in PC, which in turn functions as the acyl donor for TAG synthesis [23]. This pathway provides the bulk of TAG synthesis in developing leaves, while DGAT is more active during leaf senescence [24]. A third enzyme catalyzing the acylation of phytol during leaf senescence or stress in *Arabidopsis thaliana*, phytyl ester synthase (PES), was recently characterized with DGAT bifunctionality ex vivo, making PES the only known chloroplastic DGAT [25]. Adding to the complexity of TAG synthesis are acyl-editing reactions and remodeling of membrane lipids [26,27].

Recently, we discovered a divergence in activities of the prokaryotic (chloroplastic) and eukaryotic (ER) TAG metabolic pathways between algae of the classes *Chlamydomonadales*, *Chlorophyceae* and *Trebouxiophyceae* [28]. This exemplifies that, while much is currently known about the pathways of TAG synthesis in *C. reinhardtii*, there is a scarcity of information in other algae. This research presented here represents the first steps in determining the mechanism of TAG synthesis in *Coccomyxa subellipsoidea* C-169. This strain was isolated from Marble Point, Antarctica and may offer adaptive strategies, particularly at low temperatures, for TAG and other lipid production and thus serve as an ideal feedstock for biofuel production. The work detailed in this study represents the first steps required to address the metabolic changes leading to increased TAG synthesis in *C. subellipsoidea* C-169. Following ten days of N starvation, as expected, there was increased TAG synthesis with a commensurate loss of chloroplast membrane lipids. A key finding from this work was that the increased levels of TAG largely come from de novo fatty acid synthesis and, as with plants, a significant number of acyl groups were transferred from membrane lipid pools. With the re-addition of N, the TAG pool is rapidly degraded and the resultant acyl chains serve as substrates for the synthesis of galactolipids. These results suggest a distinct metabolic program is induced by N stress and is defined by changes in fatty acid synthesis, the relative contributions of membrane lipid acyl chain recycling, and the relative activities of the chloroplast and endoplasmic reticulum LPATs.

2. Materials and methods

2.1. Bioreactor growth conditions

C. subellipsoidea C169 was a gift from Dr. James Van Etten (University of Nebraska–Lincoln). The initial inoculum was grown for one week in 50 mL cultures. These cultures were centrifuged, cell pellets resuspended in 200 mL of fresh Bolds basal medium (BBM), and added to a sterile, round, water jacketed 3 L glass bioreactor (Applikon Biotechnology, Foster City, CA) to a final volume of 2 L. The culture was grown photoautotrophically with 200 μmol photons m^{-2} s^{-1} at 25 °C and mixed using an impeller with two Rushton turbine blades and three baffles. A thermocirculator was used to maintain a constant temperature in the bioreactor by circulating water through the jacket. Bubbling compressed air through a 0.2 mm polytetrafluoroethylene (PTFE) filter provided 330 ppm CO_2 at 1 L min^{-1}; the pH was maintained at 6.6 using 0.1 M KOH and 0.1 M HCl. The pH was monitored using an autoclavable pH electrode (Applikon Biotechnology Inc., USA). Air input, temperature and pH were continuously recorded using the BioXpert software from Applikon and never varied. The culture was collected after five days of growth by centrifugation and suspended in 200 mL of BBM media with no N source added (N-BBM), which was added to 1.8 L of N-BBM in the bioreactor. The bioreactor was slightly pressurized from the air input, and opening an external valve allowed for the sterile removal of samples by displacement through a stainless steel tube with an open end 2 in. from the bottom. 80 mL aliquots were collected at 24 h intervals, chilled immediately on ice, subdivided, centrifuged, and the cell pellets stored at −80 °C until use as detailed below. Three pellets from each time point were lyophilized and the dry weights (DW) determined. As is standard for bioreactor experiments with continuous monitoring [29], the data presented is from one representative experiment, of three biological replicates. The data presented represent the mean ± standard error of the mean (SEM) or standard deviation (SD) as noted with an n= 3–5.

2.2. Confocal microscopy using Nile Red and chlorophyll determination

The development and degradation of lipid droplets was visualized using the lipophilic fluorophore Nile Red (Sigma) according to Chen et al. [30] with minor changes. Briefly, algal pellets corresponding to 1 mL of cells with an optical density of 2.0 at 550 nm were suspended in 0.5 mL of 50 μM Nile Red in 3:1 aqueous DMSO and stained for 30 min at 37 °C in a shaking incubator. Fluorescence images were collected using a laser scanning confocal microscope (Olympus FluoView 500). Chlorophyll concentration was measured during the bioreactor time course as a proxy for changes in photosynthetic capacity and chloroplast integrity. Briefly, bioreactor culture was collected and cell density measured by absorbance at 550 nm. Chlorophyll was extracted immediately from 1 mL of culture into 1 mL of methanol after homogenization and cellular debris removed by centrifugation. The sample was measured by UV in a quartz cuvette using the following equations to determine chlorophyll a (Chl a) and chlorophyll b (Chl b) concentrations:

$$\text{Chl a} = 16.29\, A^{(665.2-750.0)} - 8.54\, A^{(652.0-750.0)}$$

$$\text{Chl b} = 30.66\, A^{(652.0-750.0)} - 13.58\, A^{(665.2-750.0)}$$

2.3. Lipid standards and extraction

Internal standards used in quantifying lipids were as follows: 1,2,3-triheptadecanoyl-*sn*-glycerol (Nu-Chek Prep, Elysian, MN), 1,2-diheptadecanoyl-*sn*-glycero-3-phosphocholine, 1,2-diheptadecanoyl-*sn*-glycero-3-phosphoethanolamine, and 1,2-diheptadecanoyl-*sn*-glycero-3-phospho-(1′-rac-glycerol) (Avanti Lipids, Alabaster, AL). Monogalactosyl-diacylglyceride (MGDG) and digalactosyl-diacylglyceride (DGDG) standards were quantified using internal standards with known stearoyl and stearoyl/palmitoyl compositions (Matreya LLC, Pleasant Gap, PA). Endogenous saturated galactolipid content was determined to be negligible during unlimited and N-starved growth. Triplicate samples were extracted with methanol/chloroform (2:1) containing 0.01% butylated hydroxytoluene (BHA; Sigma-Aldrich) using a bead mill (Qiagen TissueLyser LT, Qiagen, Valencia, CA) set to 50 Hz for 5 min. A slightly modified method of the Bligh and Dyer [31] technique for total lipid extraction was employed. Briefly, bead mill disrupted cells in chloroform/methanol (2:1) were incubated at room temperature for 1 h on a multi-vial vortexer. Lipids were partitioned by adding 1 mL of chloroform and 2 mL of 0.8% aqueous potassium chloride solution followed by a brief vortexing step and centrifugation for 5 min at 2520 ×*g*. The organic phase was removed to a fresh vial and evaporated under nitrogen gas. The sample was finally dissolved in into methanol/chloroform (1:1).

2.4. Trans-methylation and GC–MS analysis of complex lipids

Fatty acid methyl esters (FAMEs) were synthesized from lipid extracts using a modification of the method published by Morrison and Smith [32]. Briefly, extracts were saponified for 5 min at 100 °C in 0.5 mL 0.5 M potassium hydroxide in methanol; the samples were allowed to cool and 0.5 mL of boron trifluoride (14% in methanol) was added, which were again heated to 100 °C for 5 min. Extracts were kept under a headspace of argon throughout the process. Solvent partitioning with 0.5mL of hexane and 1mL of saturated aqueous sodium chloride solution was used to separate and purify the FAME mixture. Partitioning was aided by centrifugation (2000 ×*g*; 5 min). The hexane layer was isolated and FAMEs analyzed directly by GC–MS using an Agilent 7890A GC and a 5975C VL MS triple axis detector (Agilent Technologies, Santa Clara, CA). The column used was an Agilent CP7421 Select FAME (200 m × 271 μm × 0.25 μm). The oven temperature was set at 130 °C for 10 min, ramped by 10 °C min^{-1} to 160 °C and held for 7 min. The temperature was ramped again at 10 °C min^{-1} to 190 °C, held 7 min, then increased again by 10 °C min^{-1} to 220 °C and held for 22 min. A final temperature of 250 °C was reached by an increase of 10 °C min^{-1} and held for 17 min. The pressure was held constant at 62.3 psi and the inlet temperature set to 250 °C. Peaks were evaluated by fragment analysis against a standard NIST database and verified using a mixture of authentic standards (37 FAME standard; Fisher Scientific). The mol% of each was calculated by comparison with a standard of known amount (heptadecenoic methyl ester). The data presented represent the mean ± standard error of the mean (SEM) or standard deviation (SD) as noted with an n = 3–5.

2.5. Quantification of complex lipids by LC–MS/MS

Complex lipids were analyzed using a SCIEX Q-Trap 4000 LC–MS/MS coupled to a Shimadzu UFLC-XR system and an Agilent Poroshell 120 EC-18 4.6 × 50 mm (2.7 μm) column and an Agilent Eclipse Plus-C18 narrow bore 2.1 × 12.5mm(5 μm) guard column (Agilent Technologies, Santa Clara, CA) varying binary solvent systems. In general, lipid extracts equivalent to 1 × 105 cells were injected. Mono-, di-, and trigalactosyl-diacylglycerides were analyzed using 95:5 methanol/water/1.6 mM ammonium formate/0.7 mM formic acid (Solvent A) and methanol/ 1.6 mM ammonium formate/0.7 mM formic acid (Solvent B). The gradient increased with a column temperature of 30 °C from 0 to 100%. Solvent B in 6 min, held for 4 min, decreased to 0% in 0.5 min, and held for 1.5 min. An Agilent Pursuit 5 PFP 150 × 2.0 mm column was used for phospholipid separations (Agilent Technologies, Santa Clara, CA). Phosphatidylcholines, phosphatidylethanolamines, and phosphatidylglycerols were analyzed using 70:5:25 methanol/ isopropanol/10 mM aqueous ammonium formate (Solvent A) and 94:5:1 methanol/isopropanol/10 mM aqueous ammonium formate (Solvent B). The gradient was run at a column temperature of 40 °C. Solvent B increased from0 to 50% in 10 min, 100% in 2min, held for 2min, then decreased to 0% in 1 min and was held there for 1 min. Triglycerides were analyzed according to the method of Allen et al. [28] and by exhaustive measurements of unsaturated TAG molecular species containing C18 and/or C16 fatty acyl chains and up to three double bonds and their resulting fragment ions. A binary solvent system consisting of methanol/1.6 mM ammonium formate/0.7 mM formic acid (Solvent A) and chloroform (Solvent B) was used for both analyses. Solvent B concentration began at 7% held for 1 min, was increased to 25% over 2 min, 30% in 4 min, then 7% in 1 min and held for 2 min. Triglycerides (TAGs) were quantified after lipid extraction were first hydrogen saturated to remove the complexity inherent to double bond quantity and placement by sealing them with 1 mg of platinum (IV) oxide (Sigma-Aldrich), replacing the head space with hydrogen gas, and vortexing for 30 min. All complex lipids were analyzed using MRMs of their ammoniated ions and their collision fragments. The data presented represent the mean ± standard error of the mean (SEM) or standard deviation (SD) as noted with an n = 3–5.

2.6. Analysis of acyl chain unsaturation of intact TAG molecular species

The method of Liu et al. [33] was used to identify and quantify TAG molecular species with the unsaturation left intact. MRM–LC–MS/MS measurements were done of all possible transitions of molecular and fragment ions for TAG species containing C18 and/or C16 fatty acids with up to three double bonds per acyl chain. Column separations were identical those already described with only the MRM transition lists altered, and TAG molecular species were quantified by comparison to a triheptadecanoate standard. A total of 240 MRM transitions were analyzed split into 6 injections of 40 transitions each. Since MRM transitions do not differentiate the site of unsaturation, many of those measured could represent multiple TAG molecular species (e.g., the MRM transition defining the TAG 18:1/18:1/16:1 is the same for the TAGs 18:1/18:2/16:0 and 18:1/18:0/16:2). 66 of the 240 MRM transitions measured were present above the 100 ppm (of dry weight algae) threshold of measurement, 32 of which represented only one TAG molecular species, 34 varied in regioisometry but had a known number of polyunsaturated fatty acyl groups, and 12 were ambiguous. These represented only 15% of the total TAG quantity and given the complexity of the data were not included in our analyses. The data presented represent the mean ± standard error of the mean (SEM) or standard deviation (SD) as noted with an n= 3–5.

3. Results

3.1. Accumulation of TAG in lipid droplets

C. subellipsoidea C-169 accumulated lipid droplets over the course of the 10-day nitrogen starvation (Fig. 1). As expected lipid droplets were visible by day 3 and increased in both size and intensity for the duration of N starvation. The addition of nitrate on day 10 was followed by a rapid reduction in lipid droplets apparent by Nile Red fluorescence after a one-day lag period.

3.2. Acyl chain composition of the triglyceride pool during nitrogen starvation

To gain key information regarding the source of the acyl chains during increased triglyceride (TAG) synthesis in N starvation, we used our recently developed LC–MS/MS method that relies on catalytic hydrogenation to remove acyl chain unsaturation and enable quantitative measurements of TAG levels [28]. Consistent with the accumulation of the lipid bodies, the TAG pool represented the most dramatic shift in lipid class quantity during N starvation. TAG increased linearly by 1.5% dry weight day^{-1} ($r^2 = 0.99$) over the 10-day period of N starvation and reached a final concentration of 96 mg L^{-1} of culture at day 10, which represented 12.8% of the dry weight (Fig. 2). The re-addition of N on day 10 resulted in a 22-fold decrease in the TAG pool to 4.3 mg L^{-1} (0.44 ± 0.01% dry weight) in a 24 h period, commensurate with a notable increase in cell growth.

We next addressed the composition of the TAG pool, with a specific focus on acyl chain length over the 10-day period of N starvation to gain insights as to whether the increase in the TAG levels was a consequence of the degradation of chloroplast membrane lipids as reported in other algal species [34] or in combination with de novo fatty acid synthesis. The initial increase of TAG accumulation (days 1–3) was proportional to specific changes in the C16/C18 acyl chain ratio, which decreased from 0.38 ± 0.02 to 0.25 ± 0.01. This ratio, which remained stable through day 10 of N starvation, was consistent with increased fatty acid synthesis culminating with C18 fatty acids (Table 1). While the C18 fatty acids were the predominant acyl chains in the

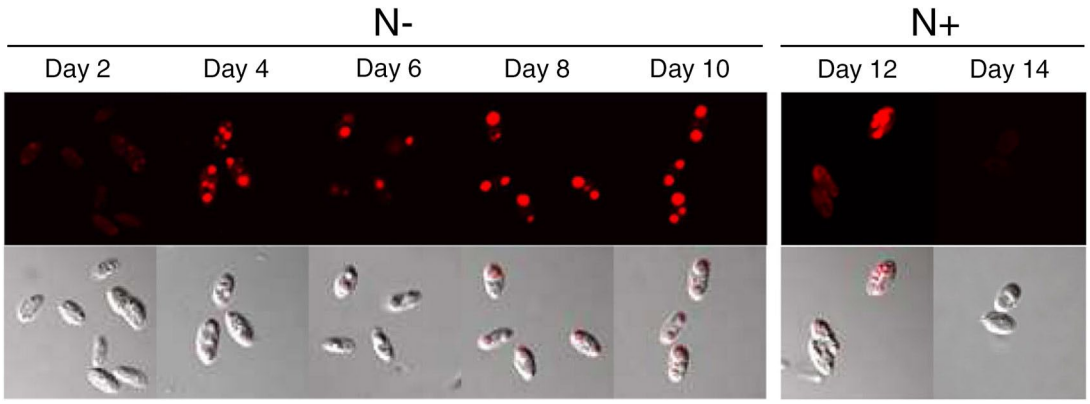

Fig. 1. Confocal microscopy of *C. subellipsoidea* showing the development and degradation of lipid droplets during N starvation and re-addition. Cells were treated with Nile Red (upper panels) and merged with Nomarski images (lower panels).

newly synthesized TAG, C16, while decreased, was proportionally increased over the N starvation period, suggesting a fixed ratio of available acyl chains coming from both de novo fatty acid biosynthesis and trafficking from membrane lipids (Table 1). C16 in the *sn*-2 position of the newly synthesized TAG decreased from 22% to 10% over the first three days of N starvation and then remained constant over the rest of the N starvation period. The %dryweight, of the 16/16/18, 16/18/16, 18/18/16, 18/16/18, and 18/18/18 TAG molecular species increased over N starvation. The 18/18/18 TAG species, for example, increased 1.5-fold during this period. In contrast, the 16/16/16 TAG species, decreased 14-fold by day 3 and remained low throughout the starvation period. The increase in TAG species containing C18 fatty acids is consistent with increased de novo fatty acid synthesis culminating with C18 fatty acids, which are directed to TAG synthesis under new steady state conditions during N starvation (Table 1).

The quantity and acyl chain composition of the TAGs were next defined for the 4-day period following N re-addition. During this recovery period, there was a 22-fold decrease in TAG content (13% to 4% dry weight). Of particular note was the 18/18/18 TAG species, which decreased by 10% over this 4-day period (Fig. 2, Table 1); the other TAG species remained essentially unchanged. These data showed the 18/18/18 TAG species are preferentially degraded almost immediately upon the re-addition of N. By day 4 after the re-addition of N, the molecular species of the significantly reduced TAG pool approached those defined under pre-N stressed conditions (Table 1).

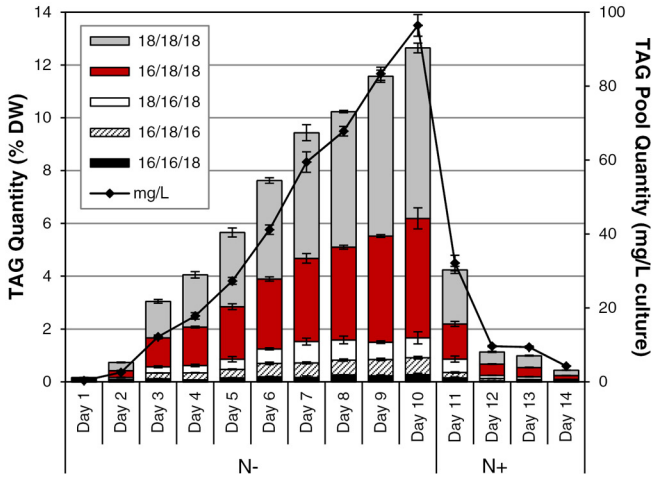

Fig. 2. Quantification of triglycerides (TAG) following catalytic saturation using LC–MS/ MS. TAG species (18/18/19 (gray); 16/18/18 (red); 18/16/18 (white); 16/18/16 (hatched); 16/16/18 (black)) were quantified as %DW algae over the 14-day bioreactor time course of 10 days in N starvation and 4 days following N re-addition; the 16/16/16 TAG species was >1% of the total TAG and not included in the figure. The black line represents total TAG quantities (mg L^{-1}). Data presented represent the mean ± standard deviation (n= 3).

It is well-documented that membrane lipids are the substrates for desaturases acting on C16 or C18 acyl chains to produce two or more double bonds in plants [35]. In *C. subellipsoidea*, these predicted desaturases share a high degree of homology with their plant counterparts supporting the notion that TAG acyl chain desaturation is a measurement for acyl chains arising from membrane lipids [35]. In order to understand the incorporation of acyl chains originating from membrane lipids, acyl chain unsaturation in the different TAG species were defined over the 10-day N starvation period using the method of Liu et al. [33]. The six most abundant TAG species were quantified using this approach, which represented 48% of the total TAG pool after 10 days of N starvation (Fig. 3A). Triolein (OOO) was the most abundant TAG species, comprising 3.0 ± 0.2% dry weight of the algae on day 10. This was more than 3-fold greater in quantity than the next abundant TAG, 1,3-dioleoyl-2-palmitoylglycerol (OPO) representing more than half of the TAG derived from DAG with C16 in the *sn*-2 position indicative of synthesis by a chloroplast-specific LPAT. The MRM data of unsaturated TAG molecular species was further analyzed to determine the rates of acyl chain redistribution from membrane lipids over the N starvation time course (Fig. 3B). The relative amounts of saturated and mono-unsaturated, di- and tri-unsaturated acyl chains were used to extrapolate the cumulative amount of these acyl groups using the quantitative assessment of TAG species by catalytic saturation (Table 1). Polyunsaturated acyl groups accumulated linearly (r2 = 0.98) in TAGs, yet rates varied in the different species (Fig. 2B). *C. subellipsoidea* contains fatty acid desaturases which are highly homologous to plant desaturases shown to have specificity for acyl chains esterified to membrane lipids. Polyunsaturated acyl chains in the TAG pool likely originated in membrane lipids and were transferred via their conversion to DAGs or free fatty acids through acyl chain editing. Over the course of N starvation, on average, 18% ± 3% of the TAG acyl chains were polyunsaturated.

3.3. Changes in chloroplast membrane lipids during N starvation and re-addition

The changes in TAG quantity and molecular species composition under N starvation conditions supported the conclusion that the acyl chains come from a combination of membrane lipid remodeling and de novo fatty acid biosynthesis. Chloroplast size reduction occurred in *C. subellipsoidea* commensurate with increased TAG synthesis during N starvation (data not shown). The chlorophyll content, as a proxy for the degradation of the photosystems, was reduced by 74% over the 10-day N starvation period (Fig. 4). Coincident with the increase in TAG

Table 1. Ratios of TAG molecular species and acyl chains by chain length. The extrapolated percentages of total TAG with C16 FA in the *sn*-2 position of the glycerol backbone are indicative of synthesis through the chloroplast-specific branch of the Kennedy Pathway (Prokaryotic Pathway).

	Days	Total TAG	Relative ratios of saturated TAG molecular species (% total)						Ratio of C16 to C18 FA	%16sn-2
		(%DW)	16/16/16	16/16/18	16/18/16	18/16/18	16/18/18	18/18/18		
N-starvation	1	0.16 (0.002)	1.38	6.91	8.44	14.37	33.86	35.05	0.38	22.2
	2	0.74 (0.02)	0.60	4.89	7.27	9.58	35.48	42.19	0.31	13.5
	3	3.05 (0.12)	0.27	3.52	7.22	7.72	35.97	45.31	0.28	10.6
	4	4.05 (0.2)	0.12	1.77	6.60	6.79	35.85	48.87	0.25	8.4
	5	5.66 (0.19)	0.14	2.47	5.76	6.79	35.15	49.69	0.24	9.8
	6	7.62 (0.24)	0.32	2.21	6.62	7.22	34.71	48.93	0.25	9.7
	7	9.44 (0.44)	0.24	1.53	5.85	8.55	33.38	50.45	0.24	9.4
	8	10.23 (0.19)	0.14	2.43	5.50	7.44	34.33	50.16	0.24	8.3
	9	11.57 (0.25)	0.14	1.85	5.32	5.66	34.72	52.30	0.23	10.4
	10	12.64 (0.39)	0.22	1.95	5.07	5.94	35.76	51.05	0.23	10.6
N-addition	11	4.24 (0.28)	0.44	3.04	4.91	11.88	31.45	48.28	0.25	15.8
	12	1.13 (0.03)	0.39	3.52	7.28	10.41	37.86	40.54	0.31	17.5
	13	0.99 (0.03)	0.45	3.64	5.40	9.91	35.75	44.85	0.28	17.8
	14	0.44 (0.004)	0.53	3.95	5.01	12.41	32.53	45.56	0.27	18.5

synthesis, these data suggest the catabolism of the plastid membrane lipids occurs in conjunction with the reduction in chloroplast size and function and that the liberated acyl chains were likely to be trafficked into the newly synthesized TAG.

To further define the sources of the acyl chains in the newly synthesized TAG, we next addressed changes in the composition of plastid membrane lipids during N starvation. ESI–MS/MS coupled with direct injection was used to assess the presence and relative amounts

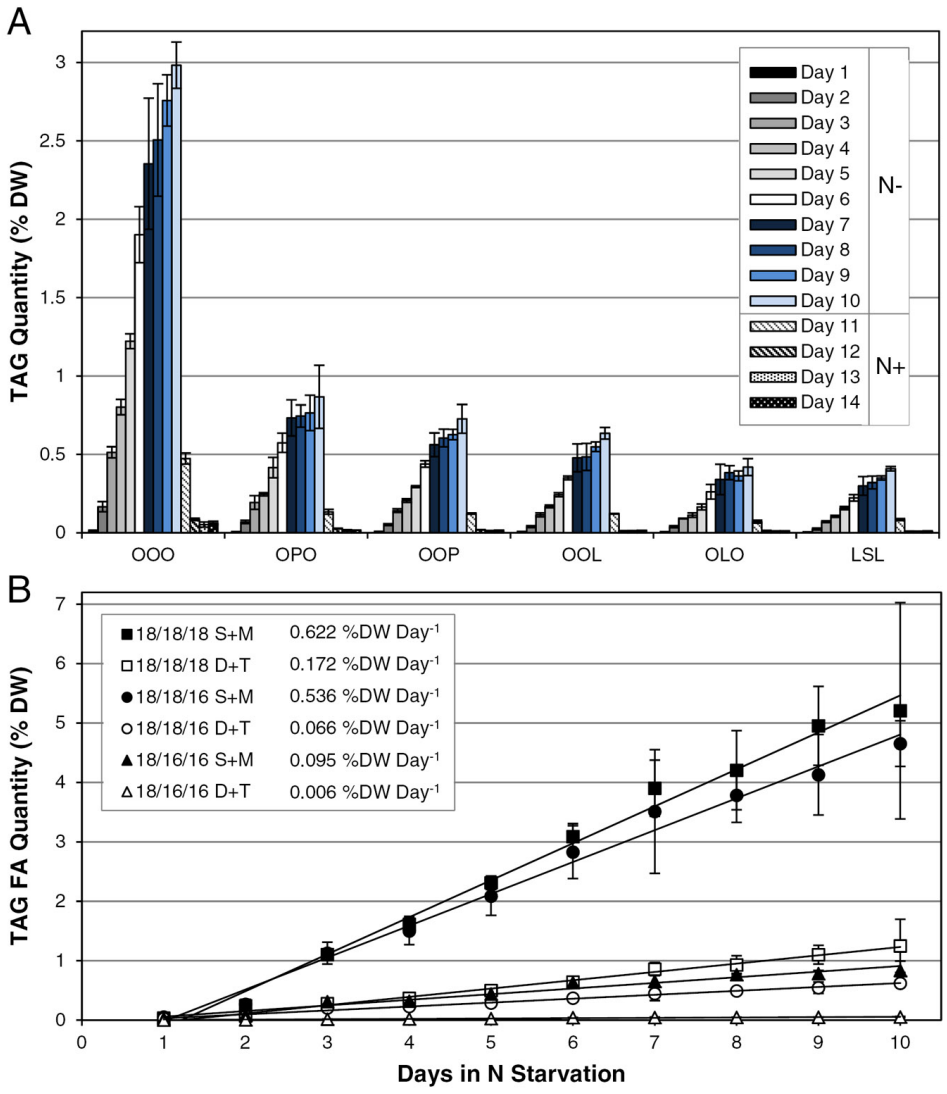

Fig. 3. Triglyceride profiling using MRM–LC–MS/MS. Total TAG pools during the time course of N starvation (days 1–10) and re-addition (days 11–14) were analyzed using multiple reaction monitoring (MRM) of all possible intact and fragment ion combinations from TAG molecules containing C18 and/or C16 fatty acids with up to three double bonds each, which represent 48% of the total TAG pool on day 10 of N starvation.

A. Changes in OOO, OPO, OOP, OOL, OLO, and LSL (O — oleic acid, P — palmitic acid, L — linoleic acid, and S — stearic acid; letters appear in order of fatty acyl chains in the *sn*-1, 2, and 3 positions) over 10 days of N starvation and 4 days of N re-addition.

B. The rates of different TAG species accumulation during N starvation (inset); the levels of saturated and monounsaturated (S + M) acyl chains are compared to the levels of di- and triunsaturated (D + T) acyl chains in the TAG pools, which likely originate from membrane lipids. The time points for each TAG species represent the mean ± standard deviation (n= 3)

of lipid classes in the chloroplast, with a specific focus on the major galactolipid species, monogalactosyl-diacylglycerol (MGDG) and digalactosyl-diacylglycerol (DGDG) (Figs. 5, 6). The chloroplast membrane lipids constituted 72% of the total complex lipids analyzed by LC–MS/MS on day 1; by day 10 of N starvation, they represented only 6% of the total complex lipid pool. The phosphatidylglycerol (PG) pool constituted 25–35% of the chloroplast lipids and its degradation paralleled the decrease in the total complex lipid pool of the chloroplast over the 10- day N starvation period. The total quantity of PG was reduced by 60% by day 10 and was essentially fully recovered after 2 days of N readdition (Fig. 5).

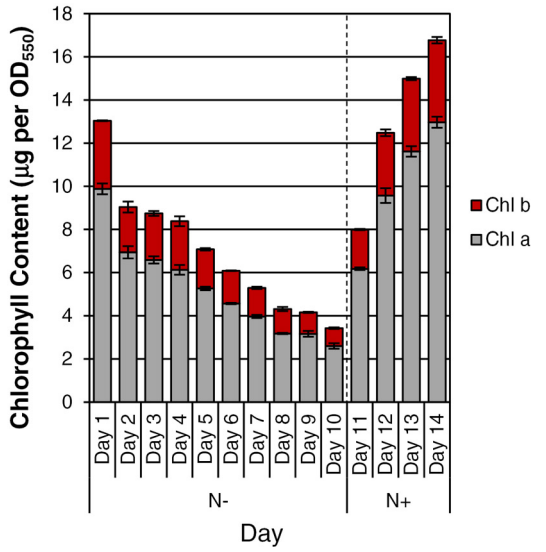

Fig. 4. Chlorophyll content during N starvation and re-addition time course. Chlorophyll a (Chl a) and chlorophyll b (Chl b) were measured by UV as detailed in Materials and methods. Data shown are the mean ± standard deviation (n = 3).

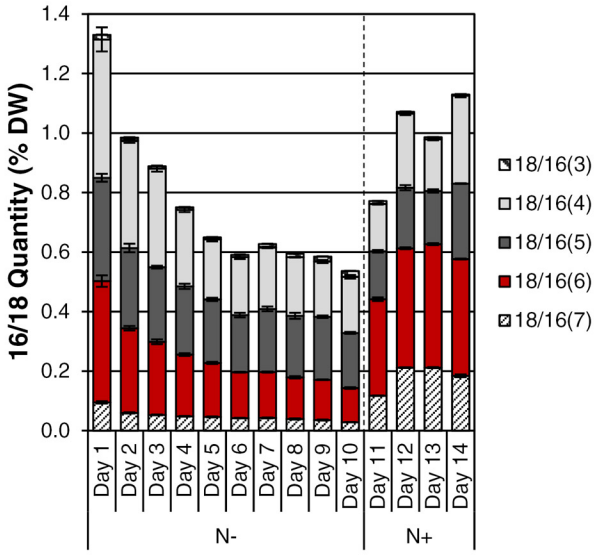

Fig. 5. Phosphatidylglycerol levels during N starvation and re-addition time course. Phosphatidylglycerol (PG) pools were quantified by MRM–LC–MS/MS over a bioreactor time course with 10 days of N starvation and 4 days of N re-addition. Molecular species are defined by the two acyl chain lengths with the total number of double bonds in parentheses (e.g., 16/18(2)) without regard to their position. Only 16/18 species were detected for this lipid class by infusion ESI–MS/MS. Data shown are the mean ± standard deviation (n = 3).

The galactolipids MGDG and DGDG, as a percentage of dry weight, were both reduced during N starvation (Fig. 6). MGDG was reduced by 78% compared to a 66% reduction in DGDG over the 10-days of N starvation. This differential reduction in DGDG and MGDG increased the relative percentage of DGDG, a bilayer forming membrane lipid, from 28% to 46% of the total galactolipid content.

The major acyl chain composition of MGDG and DGDG was 16/18 or 18/18 with varying degrees of unsaturation (1–6 doublebonds). The degree of unsaturation varied between MGDG and DGDG with MGDG, in general, being more highly unsaturated. During N starvation, the quantity (relative to %dry weight) of 16/18 MGDG with 6 double bonds (MGDG16/18(6)) did not change. However, relative to the total MGDG pool, MGDG16/18(6) increased 2-fold during the 10-day N starvation period owing to equivalent reductions in less unsaturated molecular species. The MGDG16/18 levels recovered to roughly half of pre-stressed levels following the re-addition of N; no significant changes were seen in the DGDG16/18 pools over this same period of time. Both MGDG18/18 and DGDG18/18 were found in moderate abundance and are presumed to originate either from the transfer of intact glycerolipid from extra-plastidic membranes followed by head group remodeling or direct transfer of DAG from the ER Kennedy Pathway to the chloroplast membrane. This presumption is based on studies done in plants demonstrating selective incorporation of C16 FA into the *sn*-2 position of glycerolipids by chloroplast-specific LPAT [18] and the exclusive production of 18/16 galactolipids by isolated chloroplasts [36]. The extra-plastidic origin of 18/18 galactolipids has also been shown by labeling studies of *Chlorella kessleri* [37]. During N starvation the MGDG18/18 pools increased in unsaturation, with MGDG18/ 18(6) becoming the predominate species. This finding suggests the increase in unsaturation is likely due to increased desaturase activity. By comparison, the DGDG18/18 pools remained constant in relative species quantities throughout the 10 days of N stress (Fig. 6).

The addition of nitrate on day 11 increased the MGDG18/18 and DGDG18/18 pools, suggesting essentially all of the fatty acids required for galactolipid synthesis necessary during chloroplast recovery comes from the breakdown of the 18/18/18 TAGs. Within 1 day of N readdition, the 18/18 content of MGDG and DGDG was 46% and 41%, respectively (Fig. 6C, D); the large influx of 18/18 species in the MGDG and DGDG pools coincided with the 3-fold reduction of TAG as detailed above. These data suggest a specific mechanism exists to traffic the acyl chains liberated from the 18/18/18 TAGs upon N-re-addition to immediate galactolipid synthesis. These changes were coincident with the significant greening and the 3.6-fold increase in chlorophyll content by 4 days after N re-addition. The recovery of the MGDG16/18 pools was similar to the PG pools (Figs. 5, 6); the DGDG16/18 species decreased slightly in the cells over the 4 days of N recovery (Fig. 6).

3.4. Changes in phosphatidylcholine pools during N stress and re-addition

Recent transcriptome profiling in *C. reinhardtii* demonstrated phospholipid:diacylglycerol acyltransferase (PDAT) transcripts are increased during N stress coincident with TAG accumulation [7]. This alga utilizes the betaine lipid diacylglyceryl-trimethylhomoserine (DGTS) as a primary membrane lipid and completely lacks phosphatidylcholine (PC), suggesting that PDAT may utilize DGTS in this species. Although PDAT from *C. reinhardtii* complements a genetic knock-out in yeast and can therefore use PC as a substrate, *C. reinhardtii* PDAT insertional mutants have reduced TAG pools demonstrating functionality presumably using DGTS [7]. Regardless of the ambiguity, the finding that PDAT is increased during N starvation in *C. reinhardtii* prompted us to address changes in the PC pools in *C. subellipsoidea* during N starvation and readdition to determine changes in quantity or acyl chain composition that may provide key metabolic information contributing to increased TAG synthesis. Unlike the

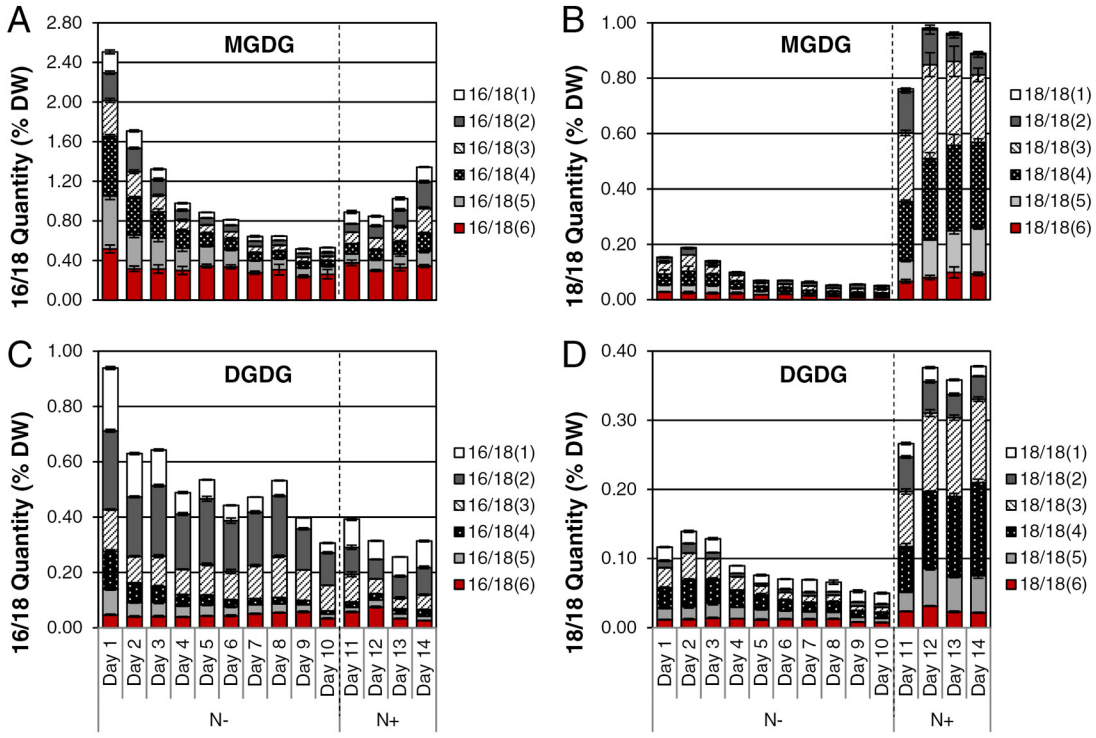

Fig. 6. Changes in galactolipid quantities during N starvation and re-addition. Monogalactosyl-diacylglycerides (MGDG) with

A. C16 and C18 fatty acids (16/18) and

B. C18 fatty acids (18/ 18) and digalactosyl-diacylglycerides (DGDG) with

C. C16 and C18 fatty acids (16/18) and

D. C18 fatty acids (18/18) were measured by LC–MS/MS during 10 days of N starvation and 4 days following N re-addition (days 11–14). Data shown are the mean ± standard deviation (n = 3).

chloroplast membrane lipids, the total quantity of PC did not change during N starvation or re-addition (Fig. 7A). The quantity of phosphatidylethanolamine (PE) was less than 5% of the PC levels and was likewise unchanged over the same time course (data not shown). While the majority of the PC species did not change over the time course of N starvation and re-addition, we found specific changes in both PC18/18 and PC16/18 suggesting their relative acyl chain quantities are important to maintain membrane lipid homeostasis. Of particular note was that N starvation resulted in a 60% decrease of PC18/18(6) by day 4, which remained constant through the starvation period; the re-addition of N increased levels just over 2-fold when compared to levels at day 1 (Fig. 7B). The same trend held for PC18/18(5) where there was an initial decrease by 35%. The readdition of N increased PC18/18(5) levels that were 15% higher than before the N starvation. Like the PC18/18 species, the three major PC16/18 species decreased beginning at day 2 of N starvation; by day 10 all three were decreased by 80–85% (Fig. 6C). The re-addition of N restored prestarvation levels of PC16/18(6). The levels of PC16/18(5) and PC16/ 18(4) had a modest increase upon N re-addition but were still 50–60% less when compared to pre-starvation levels. These data are consistent with the conclusion that PDAT is likely to function to traffic specific C16 and C18 chains from PC for TAG synthesis during N starvation. The re-addition of N resulted in a preferential increase in the PC18/18 species, which is likely coming from de novo fatty acid synthesis as would be required to expand membranes with the resumption of growth.

3.5. Quantification of total FAMEs

The experimental work detailed above demonstrated N starvation increased TAG synthesis and decreased the amounts of PG, MGDG and DGDG while having essentially no impact on PC (Fig. 7A). The different classes of lipid immediately changed following the re-addition of N and were more reflective of pre-stressed patterns. To further understand the metabolic changes during N starvation and re-addition, including the amount of total lipid, we analyzed total fatty acids using a GC–MS over the experimental time-course (Fig. 8, Table 2). Total fatty acid levels increased, as expected, in parallel with the increases noted above in total lipid quantity. A key finding from these experiments was the specific changes in $C_{16:1}^{\Delta 7}$ and $C_{18:1}^{\Delta 9}$ amounts during N starvation and re-addition. $C_{16:1}^{\Delta 7}$ decreased to levels that were at the lower limits of detection while $C_{18:1}^{\Delta 9}$ increased nearly 13-fold during N starvation. When the total fatty acid profiles were expressed in mol%, the distribution patterns of the major classes of fatty acids over N starvation and N re-addition is more apparent (Table 2). Of particular note was the increase in $C_{18:1}^{\Delta 9}$ over the 10-day N starvation period from 13 mol% to 53 mol%. The mol% of $C_{16:0}$ did not change appreciably during N starvation. By comparison the C16 monounsaturated and polyunsaturated fatty acids ($C_{16:1}^{\Delta 7}$, $C_{16:2}^{\Delta 7,10}$ and $C_{16:3}^{\Delta 7,10,13}$) decreased 3- to 10-fold in mol% over the same period. The C18 polyunsaturated fatty acids ($C_{18:2}^{\Delta 9,12}$ and $C_{18:3}^{\Delta 9,12,15}$) decreased 2-fold. This increase in $C_{18:1}^{\Delta 9}$ is presumed to come from de novo fatty acid biosynthesis and is subsequently trafficked to TAG synthesis during N starvation as opposed to galactolipid and glycerophospholipid synthesis. Following the readdition of N, the distribution of the major classes of fatty acid returned to approximately pre-stressed levels, which was coincident with the restoration of the different classes of complex lipids.

4. Discussion

4.1. Summary

In accordance with previous studies in other eukaryotic green algae, TAG accounts for nearly 75% of total lipid following 10 days of N starvation in *C. subellipsoidea*, which results from increased TAG synthesis and loss of chloroplast membrane lipids [38–40]. Fig. 9models the synthesis of TAG under N starvation conditions. The increase in TAG levels is greater than the decrease in chloroplast lipids and supports the hypothesis that fatty acids from de novo fatty acid biosynthesis account for this difference. Following 10 days of N starvation, 18% of the acyl chains in the TAG pool were polyunsaturated, which is consistent with them coming from the degradation of membrane lipids. Within the galactolipids, there is a coincident disproportional loss of MGDG compared to DGDG that is accompanied by a decrease in overall fatty acid saturation. The levels of PC are unchanged, but N

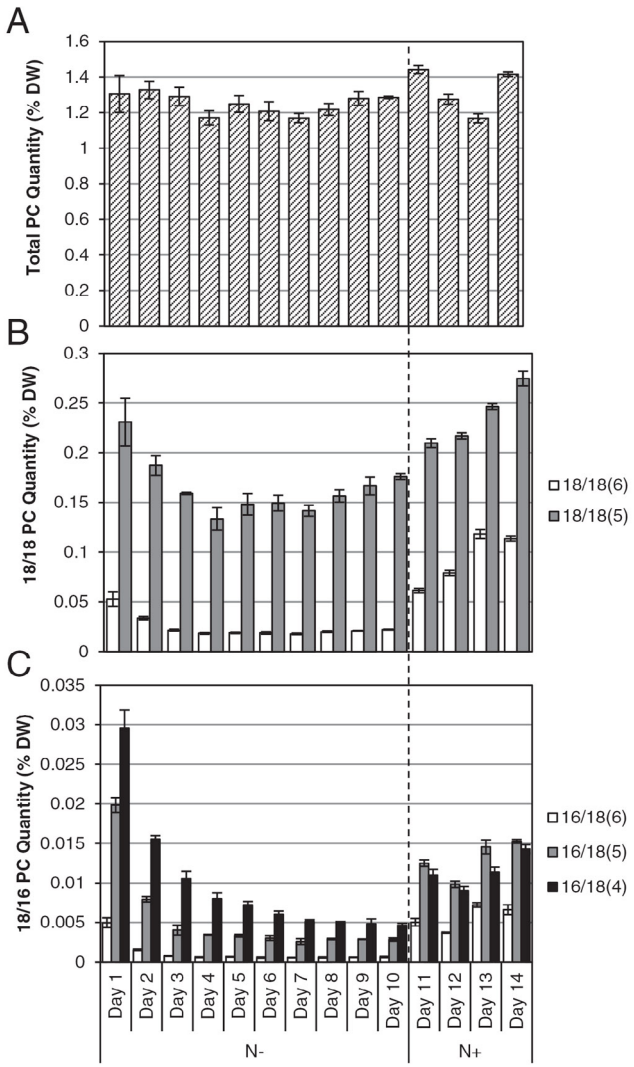

Fig. 7. Phosphatidylcholine levels and changes in unsaturated molecular species during N starvation and re-addition. Percent dry weights (%DW) of total phosphatidylcholine (PC) levels **(A)** and the more highly unsaturated PC species, 18/18(5) and 18/18(6) **(B)** and 16/18(4), 16/18(5) and 16/18(6) **(C)**. Data shown are the mean ± standard deviation (n= 3).

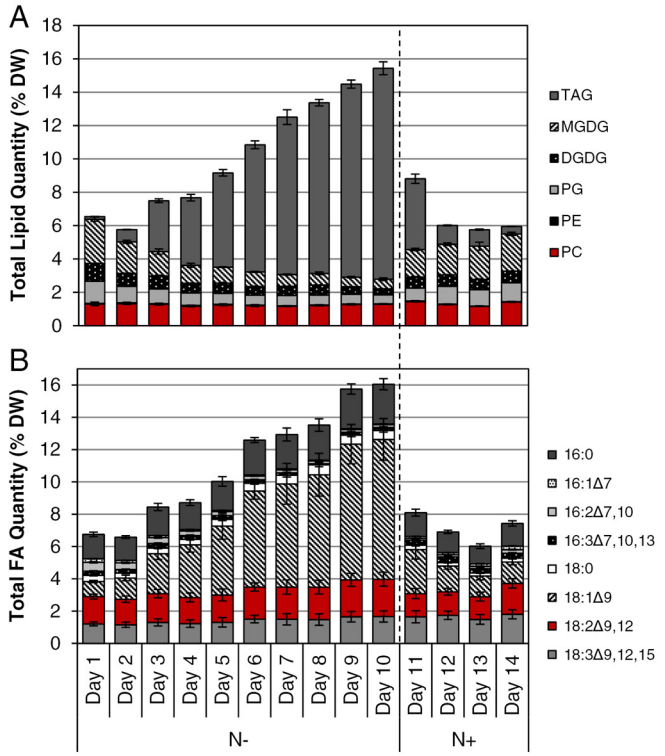

Fig. 8. Total lipid and fatty acid pools during N starvation and re-addition. **A.** Total lipid quantities determined using LC–MS/MS, and **B.** fatty acid profiles determined using GC–MS over the 14-day bioreactor time-course. The percent dry weight (%DW) presented is the mean ± standard deviation (n= 3).

stress results in moderate reductions in acyl chain unsaturation. While the incorporation of C16 and C18 fatty acids into the TAG pool during N starvation increases proportionally, $C_{18:1}^{\Delta 9}$ becomes the most abundant fatty acid, which necessarily comes from de novo fatty acid biosynthesis. The TAG pool is rapidly degraded following N re-addition and as such functions as a reservoir for the immediate synthesis of galactolipids that become enriched in the 18/18 molecular species. These studies demonstrate a distinct metabolic program is induced by N starvation and is defined by changes in fatty acid biosynthesis, membrane lipid acyl chain recycling, and the Kennedy Pathway. In total, lipid metabolism is dynamic under N starvation and re-addition as evidenced by changes in complex lipid pools consistent with a specific programmed cellular response.

4.2. TAG metabolism in C. subellipsoidea

C. subellipsoidea produced approximately the same amount of TAG during N starvation as the diatoms *Phaeodactylum tricornutum* and *Thalassiosira pseudonana*, but only one third the quantity measured in *Nannochloropsis gaditana* [38,41]. The onset of TAG catabolism occurred quickly after N re-addition and was paralleled by an increase in the 18/ 18 galactolipids. There is a nearly 2-fold increase in total galactolipid quantity during this initial 24–48 h period, which was followed by the restoration of growth with a doubling time of 2.8 days. Significant greening occurs during this initial 24–48 h period suggesting the delay in growth is related to the necessity to rebuild the photosynthetic membranes. Reducing equivalents for the assimilation of nitrate following readdition are likely to be derived from the oxidative pentose phosphate pathway rather than β-oxidation. Huppe et al. [2] reported a 2.5-fold increase in glucose 6-phosphate dehydrogenase activity in *C. reinhardtii*, indicative of oxidative pentose phosphate pathway activation, and a 70% decrease in the rate of carbon dioxide fixation when nitrate was added to N starved cells.

The difference in acyl chain length specificity between two lysophosphatidic acid acyltransferase (LPAAT) isoforms makes it possible to determine the compartment of origin of complex lipids [37]. The endoplasmic reticulum (ER) isoform preferentially adds C18 to the *sn*-2 position of lyso-phosphatidic acid to form diacylglycerol (DAG) while the chloroplast isoform prefers C16 [18]. These two reactions define the prokaryotic (chloroplastic) and eukaryotic (ER) branches of the Kennedy Pathway of complex lipid synthesis and yield DAG, which subsequently gives rise to membrane lipids or TAG. After 4 days of N starvation, approximately 10% of the newly synthesized TAG in *C. subellipsoidea* contains C16 acyl chains from chloroplastic lipids, which remains essentially unchanged during N starvation. The relative incorporation of C16 and C18 fatty acids into TAG remains essentially unchanged after three days of N starvation and re-addition (C16/C18 ratio ranged from 0.25 to 0.31). The TAG C16 and C18 chain composition in *C. subellipsoidea* is similar to that reported for *P. tricornutum* and *T. pseudonana*, that also remained the same regardless of growth stage or stress condition [41] supporting the conclusion that fatty acid chain length is an important determinant for TAG biosynthesis in algae.

Table 2. Fatty acid quantities (mol%) during N starvation re-addition. The total fatty acid profiles of *C. subellipsoidea* through 10 days of N starvation and 4 days of N re-addition were quantified by GC–MS after their conversion to FAMEs. Data presented represent the mean ± standard deviation (n= 3).

	Days	Fatty acid (mol%) ± SEM						
		16:0	16:1	16:2	16:3	18:1	18:2	18:3
N-starvation	1	22.0 (2.1)	3.3 (0.2)	8.0 (0.7)	9.5 (0.8)	13.6 (1.0)	24.7 (2.2)	17.8 (1.8)
	2	21.5 (1.2)	2.3 (0.1)	6.1 (0.5)	7.9 (0.9)	19.7 (2.6)	23.6 (2.9)	17.3 (2.5)
	3	20.7 (2.6)	1.4 (0.1)	4.3 (0.5)	7.3 (1.0)	29.0 (4.3)	20.8 (3.0)	15.2 (2.6)
	4	18.9 (2.0)	1.0 (0.1)	3.2 (0.3)	6.5 (1.0)	36.9 (5.0)	18.4 (3.1)	13.9 (2.6)
	5	17.6 (2.9)	0.7 (0.1)	2.4 (0.3)	6.5 (1.3)	41.8 (8.0)	16.6 (3.6)	12.8 (2.9)
	6	17.0 (1.2)	0.6 (0.03)	1.7 (0.2)	5.5 (0.7)	46.7 (3.9)	15.6 (2.0)	11.8 (1.8)
	7	16.2 (3.1)	0.4 (0.01)	1.5 (0.3)	5.2 (1.1)	48.9 (9.7)	15.3 (3.4)	11.4 (2.7)
	8	15.9 (2.8)	0.4 (0.02)	1.2 (0.2)	5.1 (1.0)	50.9 (9.7)	14.7 (3.1)	10.8 (2.6)
	9	15.5 (2.0)	0.3 (0.01)	1.0 (0.1)	4.7 (0.8)	52.9 (7.7)	14.4 (2.5)	10.4 (2.1)
	10	15.2 (2.1)	0.3 (0.01)	1.1 (0.05)	4.6 (0.8)	53.4 (8.0)	14.2 (2.7)	10.3 (2.1)
N-addition	11	18.0 (2.6)	1.4 (0.2)	1.4 (0.1)	7.1 (1.3)	33.2 (7.1)	17.5 (3.8)	20.0 (4.5)
	12	18.3 (1.5)	1.9 (0.1)	2.0 (0.1)	8.0 (1.0)	22.7 (2.9)	20.8 (3.0)	24.8 (3.6)
	13	17.8 (2.4)	2.5 (0.2)	2.2 (0.2)	7.6 (1.2)	21.0 (4.0)	23.0 (4.5)	24.2 (4.9)
	14	18.5 (2.2)	3.0 (0.2)	2.9 (0.3)	7.2 (0.9)	17.6 (2.4)	25.4 (3.8)	23.9 (3.7)

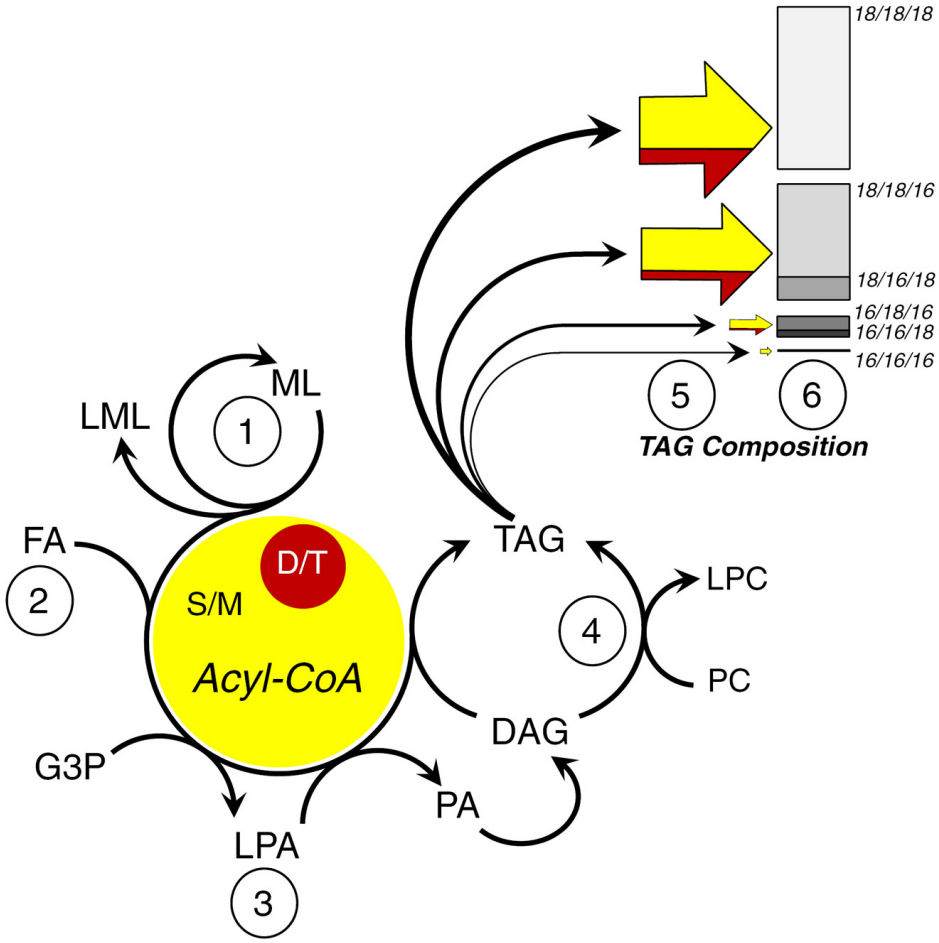

Fig. 9. Proposed model of triglyceride synthesis during N starvation in *C. subellipsoidea*. The acyl CoA precursors for TAG synthesis are derived from(1)membrane lipids (galactolipids and glycerophospholipids, ML) through acyl-editing forming a lyso-membrane lipid (LML) and (2) de novo fatty acid (FA) synthesis. (3) The sequential acylation of glycerol-3-phosphate (G3P) via the Kennedy Pathway resulting in lysophosphatidic acid (LPA) and phosphatidic acid (PA) using saturated and monounsaturated (S/M) or di- and tri-unsaturated (D/T) acyl-CoAs leads to diacylglycerol (DAG). DAG is subsequently acylated to form TAG. (4) Acyl chains are transferred directly from phosphatidylcholine (PC) to DAG forming TAG and lyso-PC (LPC) through the acyl-CoA independent enzyme, phospholipid:diacylglycerol acyltransferase. The acyl chains in the membrane lipids (ML) are further desaturated and contribute to the smaller acyl CoA pool (red),which consists of di- and tri-unsaturated species (D/T). Saturated and monounsaturated fatty acids (S/M) contribute to the larger acyl CoA pool (yellow) and come largely from de novo synthesis and to a more minor extent, membrane lipid remodeling. (5) The chain composition in the newly synthesized TAG reflects the source of the acyl- CoA (S/M, yellow and D/T, red) and consists of C18 and C16 fatty acids. In 5, the size of the arrows and color in the arrows represents the approximate amount of S/M and D/T acyl chains, respectively in the newly synthesized TAG pool. (6) The molecular species of the fatty acids in the newly synthesized TAG also differs by chain length, with approximate amounts shown for 18/18/18 (50.2% ± 1.7%), 18/18/16 (34.8% ± 1.7%), 18/16/18 (6.9% ± 2.1%), 16/18/16 (5.8% ± 0.8%), 16/16/18 (2.0% ± 0.6%), and 16/16/16 (0.2% ± 0.1%) during N starvation.

TAG biosynthesis adjusts during the first three days of N starvation, as evidenced by the 2-fold decrease of C16 fatty acids in the *sn*-2 position. This change is commensurate with 3- to 10-fold decreases in the mol% of $C_{16:1}$, $C_{16:2}$, and $C_{16:3}$, and to a lesser extent, $C_{18:2}$, and $C_{18:3}$ in the newly synthesized TAG. The reduction in $C_{16:1}$, $C_{16:2}$, and $C_{16:3}$ fatty acids in response to N starvation suggests the down-regulation of palmitate desaturation. The single palmitate-Δ^7-desaturase homolog in *C. subellipsoidea* shares 58% of sequence identity with the *A. thaliana* MGDG-specific palmitate-Δ^7-desaturase, FAD5, whose activity regulates MGDG synthesis and has been linearly correlated with the

chlorophyll content of plant leaves [42]. This loss of function is a possible factor linked to the degradation of chloroplast membrane pools, where unsaturated C16 FAs are required for complex lipid synthesis. MGDG quantity is further reduced relative to DGDG degradation during N stress in *C. subellipsoidea* and is disproportionately synthesized from 18/18 DAG precursor when N stress is alleviated. The relative proportion of chloroplast membrane lipids is known to greatly affect membrane architecture [43]. MGDG is non-bilayer forming and promotes the formation of inverted micelles during drought or freezing. Under these conditions, the remodeling of MGDG into DGDG in *A. thaliana* is mediated by the beta glucosidase-like enzyme SFR-2, with DAG and eventually TAG produced as products [44]. Although no apparent homologous genes exist in the *C. subellipsoidea* genome specifically, or outside of higher plants in general, disproportionate changes in MGDG quantity are apparent in *C. subellipsoidea* due to N stress [45].

There is evidence that algae live where changes in temperature or salinity are common, such as tidal pools and open water marine environments, the TAG pool is utilized as a storage reservoir for fatty acids required to rapidly adjust chloroplast membranes as part of normal homeostasis [39]. In the red algae *Porphyridium cruentum* eicosapentadienoic acid (EPA) synthesis occurs in the TAG pool, which is coupled to a flux mechanism exists to move those acyl chains to MGDG [46]. The EPA-deficient mutant of *P. cruentum* results in an 8-fold increase in TAG when compared to wild-type algae, suggesting the lack of EPA disrupts both influx and efflux of TAG acyl chains. A knockdown mutant of the multifunctional lipase/phospholipase/acyltransferase in the diatom *T. pseudonana* resulted in TAG accumulation under optimal growth conditions [47]. The results of these studies are consistent with a dynamic TAG pool during normal growth of algae, and that TAG accumulation is indicative of changes in the rates of influx or efflux of fatty acids through this lipid pool.

4.3. Movement of acyl chains from TAG to galactolipid pools

As noted above, the TAG pool functions as a storage reservoir for fatty acids required to rapidly adjust the properties of the chloroplast membranes [39]. In the present research, we discovered the increases in MGDG18/18 and DGDG18/18 during the recovery of chloroplast membranes after N starvation were primarily derived from 18/18/18 TAG (Fig. 4). This data suggests that *C. subellipsoidea* utilizes TAG storage as an acyl chain reservoir for galactolipid synthesis, and that this may be widespread among microalgae. In *Chlorella protothecoides* there is a reduction in membrane lipid and a proportional increase in the TAG pool during the first 12 h of N starvation, showing that the specific redistribution of acyl chains from membrane lipids is an early adaptive response [34]. This also appears to be the case for *C. reinhardtii*, where a mutation in a putative lipase, plastid galactoglycerolipid degradation 1 (PGD1), results in depressed chloroplastic membrane lipid turnover coincident with a reduction in TAG synthesis during N starvation [48]. These studies support the idea that there is a continuous flux of acyl chains through membrane lipids and into TAG pool. The difference between these species may be related to the replacement of PC with 1,2- dipalmitoyl-*sn*-glycero-3-O-4′-[N,N,N-trimethyl]-homoserine (DGTS) in *C. reinhardtii* and the apparent lack of DGTS catabolic enzymes [49]. In plants, plastoglobules are involved in thylakoid remodeling and altering specific plastoglobule proteins results in conditional chlorosis similar to N starvation [50]. Thylakoid biogenesis mutants have more numerous, enlarged plastoglobules compared to wild type as well, suggesting that these processes are linked [51]. A similar mechanism may govern the production of chloroplast lipid bodies during N starvation and their degradation upon N re-addition. We conclude that the redistribution of TAG is necessary when de novo fatty acid synthesis is suppressed by the sudden increase in free fatty acid from TAG catabolism. However, further research is needed to conclusively determine the origins of the 18/18 galactolipids and the extent of fatty acid synthesis during stress recovery.

4.4. Conclusion

The current study examines five lipid class profiles over a fourteen day, bioreactor controlled, time course of N starvation and re-addition in the model trebouxiophyceaen alga *C. subellipsoidea* using LC–MS/ MS. This is the first such quantitative analysis of global changes in complex lipids during and after abiotic stress-induced lipid body catabolism in algae, which found novel aspects of lipid metabolism. First, there is a reduction in palmitate desaturation that may account for the reduced synthesis of MGDG and related reduction in chlorophyll content. Second, the majority of the newly synthesize TAG is enriched in C18 fatty acids supporting the hypothesis that the bulk of the acyl chains come from de novo fatty acid biosynthesis. Third, a new metabolic program becomes operational under N starvation involves both chloroplast lipid synthesis and acyl chain remodeling. Collectively, this results in a fixed ratio of acyl group chain length, positioning, and double bond content in the newly synthesized TAG molecular species, which becomes stable by day 3 of N starvation and is consistent with interdependency between the different TAG synthesis pathways. Finally, the re-addition of N results in an immediate redistribution of the C18 fatty acids in TAG into membrane lipids, and especially galactolipids.

Acknowledgments — The authors thank Ronald L. Cerny and Rebecca Cahoon for technical assistance. This work was supported in whole or in part by grants from the National Science Foundation, EPSCoR Research Infrastructure Improvement Grant Track 1 (EPS-1004094 to P. N. B. and C. C. D.) and the Department of Energy (DE-FG36-08GO88055 to P. N. B.).

References

[1] G.A. Thompson, Biochim. Biophys. Acta, Lipids Lipid Metab. 1302 (1996) 17–45.

[2] H.C. Huppe, T.J. Farr, D.H. Turpin, Plant Physiol. 105 (1994) 1043–1048.

[3] F. Mairet, O. Bernard, P. Masci, T. Lacour, A. Sciandra, Bioresour. Technol. 102 (2011) 142–149.

[4] R. Tevatia, J. Allen, P. Blum, Y. Demirel, P. Black, Bioresour. Technol. 170 (2014) 152–159.

[5] A.J. Klok, D.E. Martens, R.H. Wijffels, P.P. Lamers, Bioresour. Technol. 134 (2013) 233–243.

[6] R. Miller, G.X. Wu, R.R. Deshpande, A. Vieler, K. Gartner, X.B. Li, E.R. Moellering, S. Zauner, A.J. Cornish, B.S. Liu, B. Bullard, B.B. Sears, M.H. Kuo, E.L. Hegg, Y. Shachar- Hill, S.H. Shiu, C. Benning, Plant Physiol. 154 (2010) 1737–1752.

[7] N.R. Boyle, M.D. Page, B.S. Liu, I.K. Blaby, D. Casero, J. Kropat, S.J. Cokus, A. Hong- Hermesdorf, J. Shaw, S.J. Karpowicz, S.D. Gallaher, S. Johnson, C. Benning, M. Pellegrini, A. Grossman, S.S. Merchant, J. Biol. Chem. 287 (2012) 15811–15825.

[8] D.Y. Sun, J.Q. Zhu, L. Fang, X. Zhang, Y. Chow, J.H. Liu, BMC Genomics (2013) 14.

[9] C.W. Liang, S.N. Cao, X.W. Zhang, B.H. Zhu, Z.L. Su, D. Xu, X.Y. Guang, N.H. Ye, Bioenergy Res. 6 (2013) 494–505.

[10] H.X. Lv, G. Qu, X.Z. Qi, L.N. Lu, C.G. Tian, Y.H. Ma, Genomics 101 (2013) 229–237.

[11] M.T. Guarnieri, A. Nag, S.L. Smolinski, A. Darzins, M. Seibert, P.T. Pienkos, Plos One 6 (2011) 13.

[12] J. Msanne, D. Xu, A.R. Konda, J.A. Casas-Mollano, T. Awada, E.B. Cahoon, H. Cerutti, Phytochemistry 75 (2012) 50–59.

[13] N. Wase, P.N. Black, B.A. Stanley, C.C. DiRusso, J. Proteome Res. 13 (2014) 1373–1396.

[14] C. Bolling, O. Fiehn, Plant Physiol. 139 (2005) 1995–2005.

[15] D.Y. Lee, J.-J. Park, D.K. Barupal, O. Fiehn, Mol. Cell. Proteomics 11 (2012) 973–988.

[16] T. Ito, M. Sugimoto, Y. Toya, Y. Ano, N. Kurano, T. Soga, M. Tomita, J. Biosci. Bioeng. 116 (2013) 408–415.

[17] P.D. Bates, J. Browse, Front. Plant Sci. (2012) 3.

[18] J. Browse, N. Warwick, C.R. Somerville, C.R. Slack, Biochem. J. 235 (1986) 25–31.

[19] H.-H. Guo, T.-T. Wang, Q.-Q. Li, N. Zhao, Y. Zhang, D. Liu, Q. Hu, F.-L. Li, Gene 527 (2013) 266–274.

[20] G. Banilas, M. Karampelias, I. Makariti, A. Kourti, P. Hatzopoulos, J. Exp. Bot. 62 (2011) 521–532.

[21] J.M. Shockey, S.K. Gidda, D.C. Chapital, J.C. Kuan, P.K. Dhanoa, J.M. Bland, S.J. Rothstein, R.T. Mullen, J.M. Dyer, Plant Cell 18 (2006) 2294–2313.

[22] A. Dahlqvist, U. Stahl, M. Lenman, A. Banas,M. Lee, L. Sandager, H. Ronne, H. Stymne, Proc. Natl. Acad. Sci. U. S. A. 97 (2000) 6487–6492.

[23] P.D. Bates, T.P. Durrett, J.B. Ohlrogge, M. Pollard, Plant Physiol. 150 (2009) 55–72.

[24] J.L. Fan, C.S. Yan, C.C. Xu, Plant J. 76 (2013) 930–942.

[25] F. Lippold, K. vom Dorp, M. Abraham, G. Hoelzl, V. Wewer, J.L. Yilmaz, I. Lager, C. Montandon, C. Besagni, F. Kessler, S. Stymne, P. Doermann, Plant Cell 24 (2012) 2001–2014.

[26] C. Lu, Z. Xin, Z. Ren, M. Miquel, J. Browse, Proc. Natl. Acad. Sci. U. S. A. 106 (2009) 18837–18842.

[27] I. Lager, J.L. Yilmaz, X.R. Zhou, K. Jasieniecka, M. Kazachkov, P. Wang, J.T. Zou, R. Weselake, M.A. Smith, S. Bayon, J.M. Dyer, J.M. Shockey, E. Heinz, A. Green, A. Banas, S. Stymne, J. Biol. Chem. 288 (2013) 36902–36914.

[28] J.W. Allen, C.C. DiRusso, P.N. Black, Algal Res. 5 (2014) 23–31.

[29] L. Marbelia,M.R. Bilad, I. Passaris, V. Discart, D. Vandamme, A. Beuckels, K.Muylaert, I.F.J. Vankelecom, Bioresour. Technol. 163 (2014) 228–235.

[30] W. Chen, C. Zhang, L. Song, M. Sommerfeld, Q. Hu, J. Microbiol. Methods 77 (2009) 41–47.

[31] E.G. Bligh, W.J. Dyer, Can. J. Biochem. Physiol. 37 (1959) 911–917.

[32] W.R. Morrison, L.M. Smith, J. Lipid Res. 5 (1964) 600–608.

[33] B.S. Liu, A. Vieler, C. Li, A.D. Jones, C. Benning, Bioresour. Technol. 146 (2013) 310–316.

[34] E.C. Goncalves, J.V. Johnson, B. Rathinasabapathi, Planta 238 (2013) 895–906.

[35] I.A. Guschina, J.D. Everard, A.J. Kinney, P.A. Quant, J.L. Harwood, Biochim. Biophys. Acta, Biomembr. 1838 (2014) 1488–1500.

[36] J.W.M. Heemskerk, H. Schmidt, U. Hammer, E. Heinz, Plant Physiol. 96 (1991) 144–152.

[37] N. Sato,M. Tsuzuki, A. Kawaguchi, Biochim. Biophys. Acta, Mol. Cell. Biol. Lipids 1633 (2003) 27–34.

[38] D. Simionato, M.A. Block, N. La Rocca, J. Jouhet, E. Marechal, G. Finazzi, T. Morosinotto, Eukaryot. Cell 12 (2013) 665–676.

[39] A.E. Solovchenko, Russ. J. Plant Physiol. 59 (2012) 167–176.

[40] Z.T. Wang, N. Ullrich, S. Joo, S. Waffenschmidt, U. Goodenough, Eukaryot. Cell 8 (2009) 1856–1868.

[41] E.T. Yu, F.J. Zendejas, P.D. Lane, S. Gaucher, B.A. Simmons, T.W. Lane, J. Appl. Phycol. 21 (2009) 669–681.

[42] I. Heilmann, S. Mekhedov, B. King, J. Browse, J. Shanklin, Plant Physiol. 136 (2004) 4237–4245.

[43] B. Deme, C. Cataye, M.A. Block, E. Marechal, J. Jouhet, FASEB J. 28 (2014) 3373–3383.

[44] E.R. Moellering, B. Muthan, C. Benning, Science 330 (2010) 226–228.

[45] E.R. Moellering, C. Benning, Eukaryot. Cell 9 (2010) 97–106.

[46] I. Khozin-Goldberg, H.Z. Yu, D. Adlerstein, S. Didi-Cohen, Y.M. Heimer, Z. Cohen, Lipids 35 (2000) 881–889.

[47] E.M. Trentacoste, R.P. Shrestha, S.R. Smith, C. Gle, A.C. Hartmann, M. Hildebrand, W.H. Gerwick, Proc. Natl. Acad. Sci. U. S. A. 110 (2013) 19748–19753.

[48] X. Li, E.R. Moellering, B. Liu, C. Johnny, M. Fedewa, B.B. Sears, M.-H. Kuo, C. Benning, Plant Cell 24 (2012) 4670–4686.

[49] E.I. Urzica, A. Vieler, A. Hong-Hermesdorf, M.D. Page, D. Casero, S.D. Gallaher, J. Kropat, M. Pellegrini, C. Benning, S.S. Merchant, J. Biol. Chem. 288 (2013) 30246–30258.

[50] S. Karim, M. Alezzawi, C. Garcia-Petit, K. Solymosi, N.Z. Khan, E. Lindquist, P. Dahl, S. Hohmann, H. Aronsson, Plant Mol. Biol. 84 (2014) 675–692.

[51] C. Brehelin, F. Kessler, K.J. van Wijk, Trends Plant Sci. 12 (2007) 260–266.